Nonlinear patterns dominate vegetation heterogeneity changes across spatial scales

Hu, J.; Veldhuis, M.P.; Snoo, G.R. de; Si, Y.

Nonlinear patterns dominate vegetation heterogeneity changes across spatial scales

Jie Hu[1], Michiel Veldhuis[1], Geert R.de Snoo[1,2], Yali Si[1*]*

1 Institute of Environmental Sciences (CML), Leiden University, 9518, 2300 RA Leiden, the Netherlands

2 Royal Netherlands Academy of Arts and Sciences (KNAW), Kloveniersburgwal 29 1011 JV Amsterdam, The Netherlands

*** Corresponding Author:**

Jie Hu

Email: j.hu@cml.leidenuniv.nl

Yali Si

Email: y.si@cml.leidenuniv.nl

Abstract:

Vegetation heterogeneity, is a key driver of biodiversity by providing niches and refuges and facilitating coexistence and diversification. Because heterogeneity is scale-dependent, quantifying how it varies across spatial scales is essential for understanding biodiversity patterns and guiding ecosystem management. However, empirical evidence describing how heterogeneity changes with scale remains limited. We systematically analysed 60 relationships between vegetation heterogeneity and spatial scale across three common landscape types, using six vegetation structural and one plant diversity measures and three calculation methods. We identified dominant forms of heterogeneity–scale relationships and assessed how vegetation measures, calculation methods, and landscape types influenced model support, rate of change, and characteristic spatial scales. Most relationships (88%) were nonlinear, and logarithmic models were the most common best-supported form. Maximum rates of change occurred mainly at finer spatial scales, whereas levelling-off points in logarithmic relationships were concentrated primarily below 10 km. Both slope magnitude and levelling-off scale varied significantly among vegetation heterogeneity measures, and levelling-off scale also differed among landscape types, with urban landscapes tending to level off at finer scales than agricultural and semi-natural landscapes. Overall, our results show that vegetation heterogeneity usually changes nonlinearly across spatial scales and that the scale dependence of these patterns varies among heterogeneity measures and landscape contexts. Our framework provides a useful workflow for quantifying heterogeneity–scale relationships and guiding

the selection of ecologically relevant metrics and spatial scales for biodiversity monitoring, conservation planning, and ecosystem management.

Keywords: Environmental heterogeneity, heterogeneity measurement, vegetation structure, vegetation height, vegetation richness, LiDAR data, scale-dependent, landscape

非线性模式主导植被异质性跨空间尺度的变化

摘要

植被异质性可为生物提供生态位和庇护所，并促进物种共存与分化，因此被认为是驱动生物多样性的关键因素。由于异质性具有空间尺度依赖性，因此理解其在不同空间尺度上的变化对于提高生物多样性和指导生态系统管理至关重要。然而，植被异质性跨空间尺度变化的实证证据仍然较为有限。

为识别跨空间尺度下植被异质性－尺度关系的主导模式，评估使用不同植被指标、计算方法和景观类型在对异质性－尺度关系的影响。本研究采用了6个植被结构指标、1个植物多样性指标以及3种异质性计算方法系统地分析了三类常见景观类型中植被异质性与空间尺度(本研究中尺度特指粒度)之间的60组关系。

结果表明，跨空间尺度下植被异质性－尺度关系的主导形式(88%)呈现非线性，其中对数模型是最常见的最优支持形式。最大变化速率主要出现在较细的空间尺度，而对数关系中尺度对植被异质性的影响主要集中在10km以下。植被异质性各指标随空间尺度的变化的尺度陡峭区间和平缓区间均存在显著差异；不同景观类型之间，平缓区间也存在显著差异，与农业景观和半自然景观相比，城市景观通常在较细尺度上达到平缓。

总体而言，植被异质性跨空间尺度主要呈非线性变化，而且这种尺度依赖的变化模式会因使用的植被异质性指标和景观背景不同而变化。本研究提出的分析框架为量化不同区域植被指标的异质性－尺度关系提供了可参考的工作流程,为生物多样性监测、保护规划和生态系统管理中选择生态学相关指标与空间粒度提供了指导。

关键词：环境异质性；异质性度量；植被结构；植被高度；植被丰富度；LiDAR数据；尺度依赖；景观

Introduction

Biodiversity is crucial for human wellbeing, but is projected to globally decrease in the coming decades due to human activities (Díaz *et al.* 2019; Mori 2020; Paul *et al.* 2020; Jaureguiberry *et al.* 2022; Shin *et al.* 2022). A substantial number of species from various taxonomic groups are now at risk of extinction (Worm *et al.* 2006; Leclère *et al.* 2020; Legge *et al.* 2023). This situation calls for effective strategies to bend the curve of biodiversity loss (Leclère *et al.* 2020).

Environmental heterogeneity is a key driver of biodiversity and refers to the complexity of the environment (August 1983; Hortal *et al.* 2009; Poggio, Chaneton & Ghersa 2010; Stein, Gerstner & Kreft 2014; Loke & Chisholm 2022; do Carmo Pônzio *et al.* 2024). Environmental heterogeneity contributes to biodiversity by providing diverse niches and shelters and by increasing the probability of speciation events (Simpson 1949; MacArthur, MacArthur & Preer 1962; Tews *et al.* 2004; Allouche *et al.* 2012; Stein, Gerstner & Kreft 2014; Stein 2015). These effects are expected to change across spatial scales, because environmental heterogeneity is scale-dependent (Kumar, Stohlgren & Chong 2006; Stein, Gerstner & Kreft 2014; Loke & Chisholm 2022).

Spatial scale has multiple dimensions, but in this study we use the term specifically to refer to spatial grain size, that is, the size of the analysis units, while keeping the spatial extent of the study area constant (Stein, Gerstner & Kreft 2014; Stein & Kreft 2015). Higher

levels of environmental heterogeneity have been documented at coarser spatial scales because larger analysis units may encompass a greater degree of environmental variability (Van Rensburg, Chown & Gaston 2002; Kallimanis *et al.* 2008; Stein, Gerstner & Kreft 2014). Accordingly, environmental heterogeneity can show a positive relationship with increasing spatial grain size (Fig. 1 I). In general, environmental heterogeneity might decrease towards coarser scales (Fig. 1 II), because as spatial grain size increases, smaller heterogeneous patches are aggregated into larger units and fine-scale variability is increasingly averaged out. This smoothing effect reduces the detectable heterogeneity within each sampling unit (Wiens 1989; Siefert *et al.* 2012). The relationship between environmental heterogeneity and spatial scale can be either linear or nonlinear (Shen *et al.* 2004; Sarr, Hibbs & Huston 2005; Siefert *et al.* 2012; Díaz-Varela, Roces-Díaz & Álvarez-Álvarez 2016). For nonlinear patterns, environmental heterogeneity may first increase and then decrease, or first decrease and then increase, exhibiting hump-shaped and U-shaped polynomial patterns (Fig. 1 III & IV). When increasing spatial scale no longer introduces substantial additional variation, environmental heterogeneity may level off (Díaz-Varela, Roces-Díaz & Álvarez-Álvarez 2016). This results in a positive or negative logarithmic relationship (Fig. 1 V & VI).

Environmental heterogeneity is quantified based on specific environmental measures and methods. There are more than two hundred measures for quantifying environmental heterogeneity, reflecting the broad scope of the concept (Stein & Kreft 2015). These measures encompass five aspects of environmental heterogeneity: vegetation, land cover, soil, climate, and topography (Tews *et al.* 2004; Stein, Gerstner & Kreft 2014; Stein 2015;

Heidrich *et al.* 2020). Different measures reflect distinct ecological information, suggesting that heterogeneity–scale relationships may vary among measures (Tews *et al.* 2004; Lundholm 2009; Stein & Kreft 2015; Graham *et al.* 2019; Trevail *et al.* 2021). Besides the numerous measures, at least eighteen methods exist for calculating environmental heterogeneity (Stein & Kreft 2015). The methods most frequently used in recent years are the standard deviation (SD), coefficient of variation (CV), and Shannon index (Stein & Kreft 2015). Different methods may also yield different heterogeneity–scale relationships (Stein & Kreft 2015). Moreover, landscape type may also influence how environmental heterogeneity changes across scales because environmental features differ among landscapes (Bell & Lechowicz 1991; Maestre *et al.* 2003; Lundholm 2009; Ranjard *et al.* 2013; Stein, Gerstner & Kreft 2014; Weisberg *et al.* 2014; Stein & Kreft 2015). Variability in measures, methods, and landscapes can lead to different patterns in how environmental heterogeneity changes across spatial scales. Despite limited research on this issue (Shen et al. 2004; Siefert et al. 2012; Stein & Kreft 2015; Díaz-Varela, Roces-Díaz & Álvarez-Álvarez 2016), developing a comprehensive understanding will require further testing of the scale-dependency of environmental heterogeneity with real-world data (Bradbury *et al.* 2005; Bisigato *et al.* 2009; Davison *et al.* 2023; Heidrich *et al.* 2023).

In particular, such efforts should incorporate high-resolution vegetation structure, as vegetation heterogeneity is a critical aspect of environmental heterogeneity (Tews *et al.* 2004; Lundholm 2009; Stein & Kreft 2015; Farwell *et al.* 2021). The varied arrangements of vegetation, both horizontally and vertically, have a significant impact on the availability of

resources and conditions for species (MacArthur 1964; Seidel 2018; Davison *et al.* 2023; Petruželová *et al.* 2025). Emerging remote-sensing technologies such as airborne laser altimetry (also referred to Light Detection and Ranging, LiDAR) can now accurately map vegetation structure continuously over broad areas, enabling vegetation heterogeneity to be examined across spatial scales rather than being limited to measurements at species observation points (Davison *et al.* 2023; Moudrý *et al.* 2023).

In this study, we examine how vegetation heterogeneity changes across spatial scales while keeping the spatial extent of the study area constant. Using high-resolution LiDAR-derived vegetation structure data together with field-based plant richness data from the Netherlands, we address two research questions: (1) how does vegetation heterogeneity change from fine to coarse spatial grain sizes, and (2) at which spatial scales does vegetation heterogeneity change most rapidly? To answer these questions, we characterize the form of vegetation heterogeneity–scale relationships and evaluate how these relationships vary among vegetation heterogeneity measures, calculation methods, and landscape types. We hypothesize that vegetation heterogeneity will be dominated by nonlinear relationships across spatial scales, with positive logarithmic relationships expected to be most common. The steepest changes in vegetation heterogeneity will occur at fine spatial scales. This is because at the finer scale, increasing spatial grain size initially captures substantial new variation in vegetation measures, producing a rapid increase in heterogeneity. At broader scales, however, most dominant features are already

represented, so further increases in grain contribute progressively less new information, while spatial averaging increasingly smooths variation.

Methods

Study area

This study investigated how vegetation heterogeneity changes across spatial scales in the Netherlands (Fig. 2). The Netherlands contains semi-natural, agricultural, and urban landscapes within a compact extent and relatively limited climatic and topographic gradients. This relatively constrained environmental setting is advantageous because it allows scale-dependent heterogeneity patterns to be assessed across contrasting landscapes with reduced confounding from strong climatic, soil, and topographic variation. High-resolution land-cover data, LiDAR, and vascular plant observations enabled quantification of horizontal and vertical vegetation heterogeneity across a wide range of spatial scales.

Dataset

We used vegetation vertical and horizontal structure layers at 10 m spatial resolution derived from a nationwide LiDAR data product (https://zenodo.org/record/6421381) for the Netherlands (Kissling *et al.* 2022; Kissling *et al.* 2023). The LiDAR data used to produce these layers were obtained from the Actueel Hoogtebestand Nederland version 3 (AHN3, https://www.ahn.nl/), which was collected between 2014 and 2019 using airborne laser

altimetry from aircraft (for details see Supplementary Fig. S1) (Kissling *et al.* 2022; Kissling *et al.* 2023; Shi, Wang & Kissling 2025). AHN3 point clouds were normalized relative to a 1 m Digital Terrain Model, aggregated to a 10 m grid, and used to derive 25 rasterized LiDAR-derived metrics characterizing vegetation structure using the Laserchicken feature-extraction library (Kissling *et al.* 2023).

The published data product was evaluated using 100 randomly selected 10 × 10 m plots comprising 183,837 hand-labelled LiDAR points across the Netherlands. This evaluation showed a low misclassification rate for vegetation points (0.05 ± 0.19) and high accuracy of the derived LiDAR metrics (mean accuracy 0.90 ± 0.04 across 25 metrics; range: 0.87–1.00), supporting the reliability of the dataset (Kissling *et al.* 2023). The AHN3 data, pre-processed by Rijkswaterstaat (the Directorate-General for Public Works and Water Management of the Netherlands, https://www.rijkswaterstaat.nl/), were provided with ASPRS-style classes (e.g. class 1: unclassified; class 2: ground). Vegetation was primarily represented by class 1 points, while class 2 points were used for metrics requiring both vegetation and ground returns, such as pulse penetration ratio. The workflow also excluded extreme outliers during normalization and feature extraction. The data product also includes a mask layer derived from the Dutch TOP10NL cadaster dataset (https://www.kadaster.nl/zakelijk/producten/geo-informatie/topnl) identifying water bodies and human infrastructure (e.g. buildings and roads), which helps reduce potential bias from non-vegetation structures (Kissling *et al.* 2023).

From these 25 metrics, we selected six metrics representing key components of vegetation structure (Moudrý et al. 2023), including vertical structure (e.g., vegetation height percentiles) and horizontal structure (e.g., canopy cover). Metrics that directly quantify variability (e.g., standard deviation or Shannon-based structural indices) were not included, as heterogeneity was calculated separately in our study. In addition, highly correlated metrics were excluded to reduce redundancy and multicollinearity. Pairwise correlation analyses were conducted across spatial scales, and metrics with correlation coefficients $|r| > 0.7$ were not retained. The final set of six metrics therefore captures complementary aspects of vegetation structure while minimizing statistical redundancy.

We also included vascular plant richness from the Nationale Databank Flora en Fauna (NDFF) database as one aspect of vegetation heterogeneity. NDFF database (https://www.ndff.nl/) comprises observational data on vascular plants, including 7,126,896 records from 2014 to 2019. Vascular plant inventory records differed in their recorded observation area, so they were harmonized to a common spatial framework prior to analysis. To improve comparability among observations and reduce potential spatial overlap, we retained only records with an observation plot radius of ≤ 50 m. This threshold preserved approximately 99% of the observations used in the dataset while excluding records from very large survey areas. The filtered records were then assigned to a 10 × 10 m grid matching the base raster of the LiDAR-derived vegetation layers. Each plot-level

species inventory was assigned to the grid cell containing its centroid, and species richness was then calculated at the grid-cell level rather than using the original plot extents or raw occurrence counts. All subsequent scale analyses were conducted using these gridded data, which reduced the influence of variation in original plot size on scale-dependent analyses. To define different landscape types, we used the *Landelijk Grondgebruik Nederland* (LGN) 2018 land use map (https://lgn.nl/over-lgn), which classifies the Netherlands into 48 distinct land use categories with a spatial resolution of 5 m.

Calculating vegetation heterogeneity

We calculated two aspects of vegetation heterogeneity: vegetation structure heterogeneity and vegetation diversity. Six measures representing the vegetation structure and one representing vegetation diversity are included (Fig. 3, Table 2). Vegetation structure measures include mean vegetation height (MEV) which represents the average height across each pixel. Vegetation absolute height (VAH) quantifies vegetation height in 7 layers corresponding to 7 categories: less than 1m, 1 to 2 m, 2 to 3 m, 3 to 4 m, 4 to 5 m, 5 to 20 m, higher than 20 m. Vegetation foliage layers (VF), depict four layers including grasses, shrubs, trees, and tall trees based on the pre-defined height of each layer (Fig. 3). Vegetation openness (VO) measures the ratio of ground points to the total number of points within a cell, indicating the extent to which LiDAR points penetrate through the vegetation. Canopy cover (CC) was defined as the number of normalized LiDAR returns above the

mean normalized vegetation height within each grid cell. The maximum vegetation height (MAV) represents the maximum height of the tree canopy. Vegetation diversity refers to a measure of the number of vascular plant species (VS) within certain area.

We used a grid-based approach to calculate heterogeneity measures across multiple spatial scales, ranging from 0.05 to 15 km. Here, spatial scale refers specifically to spatial grain size, defined as the grid-cell size (analysis unit), which increased in 0.05 km steps from 0.05 to 0.5 km and in 0.5 km steps from 0.5 to 15 km. The overall spatial extent of the study area and the base raster's resolution were kept constant; only the grid-cell size (spatial grain) was varied. At each spatial grain, we calculated vegetation heterogeneity using three commonly used methods: Coefficient of Variation (CV), Standard Deviation (SD), and Shannon's Diversity Index (*H'*). The detailed calculations are as follows:

$$CV = \frac{\sigma}{\mu} \times 100\% \quad (1)$$

where σ is the standard deviation and μ the mean value of the vegetation measures.

$$SD = \sqrt{\frac{\sum(x_i - \mu)^2}{N}} \quad (2)$$

where x_i is the value of the lidar data of the vegetation measures at location i, μ is the mean value of these data points, and N is the number of data points.

$$H' = -\sum_{i=1}^{R}(p_i \cdot \ln p_i) \quad (3)$$

where R is the total number of categories for the vegetation measure, and p_i is the proportion represented by category i.

To calculate vegetation heterogeneity using SD and CV, we first convert the categorical measure, i.e., foliage layers, to a continuous variable (Schindler, Poirazidis & Wrbka 2008; Culbert *et al.* 2013). The original foliage layers included grass, shrub, tree, and tall tree. For each raster cell, presence/absence was recorded as binary values (1 = present, 0 = absent). A cell-level foliage richness score was calculated as the proportion of present layers relative to the total possible layers. Cells with all four layers scored 1, three layers 0.75, two layers 0.5, one layer 0.25, and no foliage 0 (Detailed description can be found in Supplementary Fig. S2). SD and CV were then calculated from these derived values. To calculate the Shannon index, we required categorized measures. We thereby converted the measures with continuous values to categorized ones using an entropy-based local indicator of spatial association in the R package *elsa* (Naimi *et al.* 2019), and the detailed information can be found in Supplementary Fig. S3.

To account for landscape context, we reclassified the LGN 2018 land cover map into three landscape types: semi-natural, urban, and agricultural landscape (Supplementary Table S1; Supplementary Fig. S1). For each spatial scale, we determined the dominant landscape type in every grid cell, defined as a landscape occupying > 90% of the cell. This scale-specific dominant landscape layer was then used to extract vegetation heterogeneity values (CV, SD, Shannon index) within each landscape type across scales. All analyses

(otherwise specified) were carried out in R 4.3.1 (R Core Team 2023) using R package *raster* (Hijmans *et al.* 2015).

Statistical analyses

We characterized vegetation heterogeneity–scale relationships in terms of overall shape, rate of change, and key transition points. For each relationship, we fitted three candidate models relating vegetation heterogeneity to spatial grain: a linear model, a logarithmic model, and a second-degree polynomial model, using the *minpack.lm* package (Elzhov *et al.* 2016). Because the number of observations differed among grains, we controlled for unequal sample sizes by randomly resampling 1000 values from grains with more than 1000 observations, while retaining all values for grains with fewer than 1000 observations. This resampling procedure was repeated 99 times.

In each iteration, sampled observations were assigned to spatial blocks based on their x and y coordinates and split into training and testing subsets using a spatial block procedure. Candidate models were fitted to the training data, and their relative support was quantified using Akaike weights derived from ΔAIC values. Predictive performance was separately assessed on held-out test data using MAE, MSE, RMSE, and MAPE. For each heterogeneity–scale relationship, the primary model was ultimately defined as the model with the highest mean Akaike weight across iterations.

For logarithmic relationships, we quantified the rate of change using the first derivative and defined a reference levelling-off scale as the scale at which the predicted changes reached 95% of the modelled maximum. For second-degree polynomial relationships, turning points were identified as the scales at which the first derivative equalled zero. For linear relationships, the slope was treated as constant across scales. To characterize the scale of most rapid change, we identified in each iteration the scale at which the absolute slope was greatest for the iteration-specific primary model, and then summarized these values across iterations. Mean observed values, fitted curves, and scale-related metrics were summarized across the 99 iterations as means and standard deviations. Model fit was further inspected using Q–Q plots, residual-versus-fitted plots, and residual histograms (Supplementary Fig. S4–S23). Residual spatial autocorrelation was assessed using Moran's I in the *spdep* package (Bivand 2022). Additional details of the resampling, model fitting, scale-metric extraction, and diagnostic procedures are provided in Supplementary, section "Methods: detailed statistical workflow".

To investigate the effects of vegetation measures, heterogeneity calculation methods, and landscape types on the change in heterogeneity across scales, we compared differences in maximum slopes and levelling-off scales among these three groups separately. We first tested the normality of data distributions using the Shapiro–Wilk test (González-Estrada & Cosmes 2019). As the data were not normally distributed, we subsequently applied the

Kruskal–Wallis test followed by Dunn's test for post hoc comparisons(Liu 2015). The analyses were carried out using the *FSA* package in R (McKight & Najab 2010; Elliott & Hynan 2011; Ogle & Ogle 2017). We then compared and the *PMCMRplus* package in R (Liu 2015; Pohlert & Pohlert 2018).

Results

The pattern of vegetation heterogeneity changes across spatial scales

Across spatial scales, most vegetation heterogeneity–scale relationships were strongly supported by nonlinear models (53 of 60 observations, 88%), 65% displayed logarithmic relationships and 23% displayed polynomial nonlinear patterns, whereas only 7 of 60 observations (12%) were most strongly supported by linear models (Fig. 4, Table 2, Supplementary Fig. S25-31). Among the seven measures used to calculate changes in heterogeneity across scales, four exhibit both linear and nonlinear patterns, while three display only nonlinear patterns. Specifically, linear patterns are observed for vegetation absolute height, vegetation foliage layer, vegetation openness, and vegetation species heterogeneity (Fig. 4, Table 2). When using the CV (21 observations) to quantify heterogeneity across scales, 81% were most strongly supported by nonlinear models (57% displayed logarithmic relationships and 24% displayed polynomial nonlinear patterns). Using the SD (21 observations), 100% were most strongly supported by nonlinear models (81% displayed logarithmic relationships and 19% displayed polynomial nonlinear patterns), and using the Shannon index (18 observations), 83% were most strongly

supported by nonlinear models (56% displayed logarithmic relationships and 27% displayed polynomial nonlinear patterns). Overall, vegetation heterogeneity–scale relationships were therefore predominantly supported by nonlinear functional forms (Fig. 4, Table 2). Nonlinear patterns consistently dominated across all landscape types (Fig. 4, Table 2), with only slight differences in their proportions: 80% in urban landscapes (20 observations, 45% displayed logarithmic relationships and 35% displayed polynomial nonlinear patterns, Fig. 4A, Table 2), 90% in agricultural landscapes (20 observations, 80% displayed logarithmic relationships and 10% displayed polynomial nonlinear patterns, Fig. 4B, Table 2), and 95% in semi-natural landscapes (20 observations, 80% displayed logarithmic relationships and 15% displayed polynomial nonlinear patterns, Fig. 4C, Table 2).

Maximum rate of change in vegetation heterogeneity across spatial scales

Among the 53 observations for which nonlinear models received the strongest support, 91% of the maximum rates of change in vegetation heterogeneity occurred at finer spatial scales (< 5 km; Fig. 4, Supplementary Table S2). The location of the steepest slope along these nonlinear curves differed significantly among heterogeneity measures ($P = 0.033$), but not among calculation methods ($P = 0.308$) or landscape types ($P = 0.692$; Fig. 5). Across measures, maximum vegetation height showed higher maximum slope values than vegetation foliage layer, and this pairwise difference was significant ($P < 0.05$; Fig. 5A). In

contrast, maximum rates of change did not differ significantly among heterogeneity calculation methods or landscape types (Fig. 5B, C).

Turning points in vegetation heterogeneity change across spatial scales

Among the 39 datasets for which the logarithmic model received the strongest support, levelling-off points of vegetation heterogeneity occurred across a broad range of spatial scales but were still concentrated mainly below 10 km (Supplementary Table S2). Of these logarithmic relationships, 8% levelled off before 0.5 km, 36% between 0.5 and 5 km, 26% between 5 and 10 km, and 31% between 10 and 15 km. The scales at which heterogeneity levelled off varied significantly across the measures analysed ($P = 0.009$; Fig. 6A). Vegetation openness levelled off at coarser scales than vegetation foliage layer and canopy cover, whereas the remaining pairwise comparisons among measures were not significant (Fig. 6A). The choice of heterogeneity calculation method did not affect the scales at which levelling-off occurred ($P = 0.129$; Fig. 6B). Levelling-off scales differed significantly among landscape types ($P = 0.021$; Fig. 6C). Urban landscapes exhibited finer levelling-off scales than agricultural and semi-natural landscapes, whereas the latter two did not differ significantly from each other. Among the 14 datasets for which the second-degree polynomial model received the strongest support, most heterogeneity–scale relationships exhibited turning points at relatively fine spatial scales. Of the 13 datasets with identifiable turning points within the observed scale range, 69% reached their turning points below 5

km, 8% between 5 and 10 km, and 23% between 10 and 15 km. One polynomial relationship did not show a turning point within the observed scale range.

Discussion

This study investigates changes in vegetation heterogeneity across spatial scales by comparing seven measures, three calculation methods, and three landscape types. Across datasets, most vegetation heterogeneity–scale relationships were nonlinear, with only a minority showing linear trends. Among the nonlinear forms, logarithmic patterns were predominant. Relationship form, slope magnitude, and levelling-off scales differed among heterogeneity measures, and also varied among landscape types. Overall, levelling-off occurred mainly below 10 km.

Among datasets with strongest support for logarithmic relationships, positive logarithmic trends predominated. Positive logarithmic trends likely occur because enlarging the analysis unit initially incorporates additional vegetation variability, leading to a rapid increase in measured heterogeneity at finer scales (Kallimanis *et al.* 2008; Stein, Gerstner & Kreft 2014). At coarser scales, however, most distinct features are already captured within the sampling units, so further increases in grain size add relatively little new variation, producing a levelling-off pattern (Smith & Lundholm 2012; Graham *et al.* 2019). In contrast, a negative logarithmic relationship may occur when key vegetation features are already present at finer scales. As the grid size increases, spatial averaging reduces

between-grid variability, resulting in a decline in heterogeneity. Because most local variation has been smoothed out, the heterogeneity trend plateaus, forming a negative logarithmic relationship (Auestad, Rydgren & Økland 2008; Smith & Lundholm 2012).

Unlike logarithmic relationships, which retain the same overall direction while approaching saturation, polynomial relationships are characterized by a turning point at which the direction of heterogeneity change reverses. A smaller subset of these nonlinear relationships followed hump-shaped patterns across spatial scales. In these cases, heterogeneity initially increased with scale as additional vegetation features were incorporated, resembling the early phase of a logarithmic relationship (Smith & Lundholm 2012; Stein, Gerstner & Kreft 2014). However, after the turning point, vegetation heterogeneity reaches its maximum, indicating the greatest variation among vegetation features (Kumar, Stohlgren & Chong 2006). With further coarsening of scale, fine-scale variation becomes increasingly obscured due to a spatial averaging effect (Sarr, Hibbs & Huston 2005; Dufour *et al.* 2006; Bisigato *et al.* 2009; Stein, Gerstner & Kreft 2014). This process ultimately leads to a decline in measured heterogeneity at coarser scales (Dufour *et al.* 2006; Smith & Lundholm 2012; Graham *et al.* 2019). In contrast, U-shaped polynomial relationships exhibit the opposite pattern. Here, heterogeneity is highest at finer scales but decreases with increasing scale as local features become spatially homogenized through averaging (Dufour *et al.* 2006). Beyond a certain threshold, however, additional increases in scale incorporate new and distinct vegetation features, enhancing spatial variability again and producing the upward turn of the U-shaped trend. Additionally,

linear relationships may indicate that heterogeneity has not yet reached a point of diminishing returns or, alternatively, that such a threshold occurs at a scale too fine to be detected within the examined spatial range (Dufour *et al.* 2006; Smith & Lundholm 2012; Loke & Chisholm 2022).

The scale at which heterogeneity changes most rapidly indicates the transition point in the heterogeneity–scale relationship. Because each measure captures distinct aspects of vegetation structure, composition, or diversity, their changes vary across spatial scales, resulting in measure-specific characteristic spatial scales (Rescia *et al.* 1997; Kumar, Stohlgren & Chong 2006; Pottier, Bédécarrats & Marrs 2009; Davison *et al.* 2023). Previous studies similarly show that plant richness and vegetation structural attributes exhibit different characteristic spatial scales (Dufour *et al.* 2006; Kumar, Stohlgren & Chong 2006; Davison *et al.* 2023). For both logarithmic and polynomial forms, these transition points indicate where the heterogeneity-scale relationship begins to level off or reverse. These transition points are measure-dependent and commonly occur at scales below 10 km (Supplementary Table S2). Turning points tend to appear at finer spatial scales, likely because many vegetation measures are most sensitive to variation at these scales. For instance, canopy cover heterogeneity has been shown to vary most strongly between 0.05 and 0.5 km, resulting in transition points at relatively fine scales (Graham *et al.* 2019). In contrast, vegetation richness, which is more influenced by regional and site-level factors, typically exhibits broader sensitive scales, with transition points occurring at coarser spatial scales (Smith & Lundholm 2012). Notably, most levelling-off points occur at finer

scales in our study, but their positions differ among landscape types. In urban areas, levelling-off occurs at finer spatial scales than in agricultural or semi-natural landscapes, indicating that vegetation heterogeneity reaches saturation earlier in urban matrices. This likely reflects the limited amount and compositional diversity of vegetation within urban matrices: as spatial grain size increases, most small vegetation patches are quickly absorbed into larger grid cells dominated by similar or impervious surfaces, so additional increases in grain primarily average out the remaining within-cell variation rather than adding new vegetation features (Mitchell *et al.* 2016). Consequently, within-grain variability in vegetation structure is reduced rapidly in urban landscapes, whereas the greater compositional diversity of semi-natural landscapes allows within-grain heterogeneity to continue increasing across larger grains before eventually reaching saturation (Seiferling, Proulx & Wirth 2014).

Several limitations should be acknowledged in interpreting our results. First, the relatively constrained environmental setting of the Netherlands is both a strength and a limitation of this study: it reduces strong climatic, soil, and topographic confounding, allowing vegetation heterogeneity–scale relationships to be identified more clearly, but it also means that the quantitative scale values reported here should be interpreted as a useful reference baseline for understanding how scale influences vegetation heterogeneity. Importantly, the identified scales represent statistical transition points in vegetation heterogeneity measured across spatial scales, rather than direct inference about ecological processes. Therefore, any ecological interpretation linking these scales to

species responses requires further empirical validation. Second, although high-resolution LiDAR data, infrastructure masks, and validation procedures were used, LiDAR-derived metrics may still underrepresent understory vegetation structure because fewer laser returns are obtained below the canopy. Third, some residual uncertainty remains in the vegetation species data because the original survey plots varied in size before being standardized to a common raster framework. Future studies could build on this reference by testing the observed relationships across broader environmental settings, improving below-canopy representation with higher point-density LiDAR, voxel-based analyses, and higher-resolution ancillary data, strengthening field sampling with more consistent plot size and survey design.

In conclusion, vegetation heterogeneity across spatial scales is predominantly characterized by logarithmic patterns, with the steepest changes occurring at finer spatial scales. Vegetation heterogeneity is scale-dependent and the relationships are influenced more by vegetation measures and landscape types than by the heterogeneity calculation methods. Despite the general nonlinear patterns, the variations in heterogeneity-scale relationships identified here further highlight that spatial context fundamentally shapes how vegetation heterogeneity emerges, reinforcing the importance of accounting for scale dependence when comparing ecological patterns across contrasting landscapes. Our results suggest that the choice of spatial scale can strongly influence measured vegetation heterogeneity and may consequently affect inferred heterogeneity–diversity relationships. For ecological monitoring and assessment, it is therefore essential to (i) select fine spatial

scales that capture the sensitivity of vegetation heterogeneity measures and are ecologically relevant to the target community, and (ii) match heterogeneity indicators to the spatial scales at which organisms in the targeted community perceive and respond to their environment. Incorporating such a scale-explicit framework into biodiversity assessments will enhance the reliability of heterogeneity metrics as indicators of ecological condition and support more effective, evidence-based conservation and land-use planning.

Authors' Contributions

Jie Hu, Michiel Veldhuis, Geert de Snoo, and Yali Si conceived and designed the study. Jie Hu drafted the first manuscript, and all authors provided insights and contributed substantially to revising the drafts.

Funding

Jie Hu acknowledges final project support from the China Scholarship Council (CSC, No. 202206180010). The project was also supported by the CML Impact Fund of Leiden University.

Acknowledgements

We sincerely thank Peter van Bodegom for his assistance with data analyses and Yifang Shi for providing valuable guidance on the use of LiDAR-based vegetation dataset. We also thank

Peng Sun for assistance with coding and Maarten van ’t Zelfde for support with data acquisition. We thank Joseph Gent for his help with English editing. Computational resources were provided by the Academic Leiden Interdisciplinary Cluster Environment (ALICE) at Leiden University.

Data Availability

The data used in this study are publicly available from open-access sources. Full details of the datasets and their access links are provided in the Methods

Conflict of interest statement

The authors declare that they have no conflict of interest.

References

Allouche, O., Kalyuzhny, M., Moreno-Rueda, G., Pizarro, M. & Kadmon, R. (2012) Area–heterogeneity tradeoff and the diversity of ecological communities. *Proceedings of the National Academy of Sciences,* **109,** 17495-17500. https://doi.org/10.1073/pnas.1208652109

Auestad, I., Rydgren, K. & Økland, R.H. (2008) Scale-dependence of vegetation-environment relationships in semi-natural grasslands. *Journal of Vegetation Science,* **19,** 139-148. https://doi.org/10.3170/2007-8-18344

August, P.V. (1983) The role of habitat complexity and heterogeneity in structuring tropical mammal communities. *Ecology,* **64,** 1495-1507. https://doi.org/10.2307/1937504

Bell, G. & Lechowicz, M.J. (1991) The ecology and genetics of fitness in forest plants. I. Environmental heterogeneity measured by explant trials. *The Journal of Ecology,* **79,** 663-685. https://doi.org/10.2307/2260660

Bisigato, A.J., Villagra, P.E., Ares, J.O. & Rossi, B.E. (2009) Vegetation heterogeneity in Monte Desert ecosystems: A multi-scale approach linking patterns and processes. *Journal of arid environments,* **73,** 182-191. https://doi.org/10.1016/j.jaridenv.2008.09.001

Bivand, R. (2022) R packages for analyzing spatial data: A comparative case study with areal data. *Geographical Analysis,* **54,** 488-518. https://doi.org/10.1111/gean.12319

Bradbury, R.B., Hill, R.A., Mason, D.C., Hinsley, S.A., Wilson, J.D., Balzter, H., Anderson, G.Q., Whittingham, M.J., Davenport, I.J. & Bellamy, P.E. (2005) Modelling relationships between birds and vegetation structure using airborne LiDAR data: a review with case studies from agricultural and woodland environments. *Ibis,* **147,** 443-452. https://doi.org/10.1111/j.1474-919x.2005.00438.x

Culbert, P.D., Radeloff, V.C., Flather, C.H., Kellndorfer, J.M., Rittenhouse, C.D. & Pidgeon, A.M. (2013) The influence of vertical and horizontal habitat structure on nationwide patterns of avian biodiversity. *The auk,* **130,** 656-665. https://www.jstor.org/stable/10.1525/auk.2013.13007

Davison, C.W., Assmann, J.J., Normand, S., Rahbek, C. & Morueta-Holme, N. (2023) Vegetation structure from LiDAR explains the local richness of birds across Denmark. *Journal of Animal Ecology,* **92,** 1332-1344. https://doi.org/10.1111/1365-2656.13945

Díaz-Varela, E., Roces-Díaz, J.V. & Álvarez-Álvarez, P. (2016) Detection of landscape heterogeneity at multiple scales: Use of the Quadratic Entropy Index. *Landscape and urban planning,* **153,** 149-159. https://doi.org/10.1016/j.landurbplan.2016.05.004

Díaz, S., Settele, J., Brondízio, E.S., Ngo, H.T., Agard, J., Arneth, A., Balvanera, P., Brauman, K.A., Butchart, S.H. & Chan, K.M. (2019) Pervasive human-driven decline of life on Earth points to the need for transformative change. *Science,* **366,** eaax3100. https://www.science.org/doi/full/10.1126/science.aax3100

do Carmo Pônzio, M., Pasqualotto, N., Zanin, M., Chiarello, A.G. & Pardini, R. (2024) Landscape heterogeneity can partially offset negative effects of habitat loss on mammalian biodiversity in agroecosystems. *Journal of Applied Ecology,* **61,** 120-133. https://doi.org/10.1111/1365-2664.14543

Dufour, A., Gadallah, F., Wagner, H.H., Guisan, A. & Buttler, A. (2006) Plant species richness and environmental heterogeneity in a mountain landscape: effects of variability and spatial configuration. *Ecography,* **29,** 573-584. https://doi.org/10.1111/j.0906-7590.2006.04605.x

Elliott, A.C. & Hynan, L.S. (2011) A SAS® macro implementation of a multiple comparison post hoc test for a Kruskal–Wallis analysis. *Computer methods and programs in biomedicine,* **102,** 75-80. https://doi.org/10.1016/j.cmpb.2010.11.002

Elzhov, T.V., Mullen, K.M., Spiess, A.-N., Bolker, B., Mullen, M.K.M. & Suggests, M. (2016) Package 'minpack. lm'. *Title R Interface Levenberg-Marquardt Nonlinear Least-Sq. Algorithm Found MINPACK Plus Support Bounds*. https://doi.org/10.32614/CRAN.package.minpack.lm

Farwell, L.S., Gudex-Cross, D., Anise, I.E., Bosch, M.J., Olah, A.M., Radeloff, V.C., Razenkova, E., Rogova, N., Silveira, E.M. & Smith, M.M. (2021) Satellite image texture captures vegetation heterogeneity and explains patterns of bird richness. *Remote sensing of Environment,* **253,** 112175. https://doi.org/10.1016/j.rse.2020.112175

González-Estrada, E. & Cosmes, W. (2019) Shapiro–Wilk test for skew normal distributions based on data transformations. *Journal of Statistical Computation and Simulation,* **89,** 3258-3272. https://doi.org/10.1080/00949655.2019.1658763

Graham, L.J., Spake, R., Gillings, S., Watts, K. & Eigenbrod, F. (2019) Incorporating fine-scale environmental heterogeneity into broad-extent models. *Methods in Ecology and Evolution,* **10,** 767-778. https://doi.org/10.1111/2041-210X.13177

Heidrich, L., Bae, S., Levick, S., Seibold, S., Weisser, W., Krzystek, P., Magdon, P., Nauss, T., Schall, P. & Serebryanyk, A. (2020) Heterogeneity–diversity relationships differ between and within trophic levels in temperate forests. *Nature ecology & evolution,* **4,** 1204-1212. https://doi.org/10.1038/s41559-020-1245-z

Heidrich, L., Brandl, R., Ammer, C., Bae, S., Bässler, C., Doerfler, I., Fischer, M., Gossner, M.M., Heurich, M. & Heibl, C. (2023) Effects of heterogeneity on the ecological

diversity and redundancy of forest fauna. *Basic and Applied Ecology,* **73,** 72-79. https://doi.org/10.1016/j.baae.2023.10.005

Hijmans, R.J., Van Etten, J., Cheng, J., Mattiuzzi, M., Sumner, M., Greenberg, J.A., Lamigueiro, O.P., Bevan, A., Racine, E.B. & Shortridge, A. (2015) Package 'raster'. *R package,* **734,** 473. https://doi.org/10.32614/CRAN.package.raster

Hortal, J., Triantis, K.A., Meiri, S., Thébault, E. & Sfenthourakis, S. (2009) Island species richness increases with habitat diversity. *The American Naturalist,* **174,** E205-E217. https://doi.org/10.1086/645085

Jaureguiberry, P., Titeux, N., Wiemers, M., Bowler, D.E., Coscieme, L., Golden, A.S., Guerra, C.A., Jacob, U., Takahashi, Y. & Settele, J. (2022) The direct drivers of recent global anthropogenic biodiversity loss. *Science Advances,* **8,** eabm9982. https://www.science.org/doi/10.1126/sciadv.abm9982

Kallimanis, A.S., Mazaris, A.D., Tzanopoulos, J., Halley, J.M., Pantis, J.D. & Sgardelis, S.P. (2008) How does habitat diversity affect the species–area relationship? *Global Ecology and Biogeography,* **17,** 532-538. https://doi.org/10.1111/j.1466-8238.2008.00393.x

Kissling, W.D., Shi, Y., Koma, Z., Meijer, C., Ku, O., Nattino, F., Seijmonsbergen, A.C. & Grootes, M.W. (2022) Laserfarm–A high-throughput workflow for generating geospatial data products of ecosystem structure from airborne laser scanning point clouds. *Ecological Informatics,* **72,** 101836. https://doi.org/10.1016/j.ecoinf.2022.101836

Kissling, W.D., Shi, Y., Koma, Z., Meijer, C., Ku, O., Nattino, F., Seijmonsbergen, A.C. & Grootes, M.W. (2023) Country-wide data of ecosystem structure from the third Dutch airborne laser scanning survey. *Data in Brief,* **46,** 108798. https://doi.org/10.1016/j.dib.2022.108798

Kumar, S., Stohlgren, T.J. & Chong, G.W. (2006) Spatial heterogeneity influences native and nonnative plant species richness. *Ecology,* **87,** 3186-3199. https://doi.org/10.1890/0012-9658(2006)87[3186:SHINAN]2.0.CO;2

Leclère, D., Obersteiner, M., Barrett, M., Butchart, S.H., Chaudhary, A., De Palma, A., DeClerck, F.A., Di Marco, M., Doelman, J.C. & Dürauer, M. (2020) Bending the curve of terrestrial biodiversity needs an integrated strategy. *Nature,* **585,** 551-556. https://doi.org/10.1038/s41586-020-2705-y

Legge, S., Rumpff, L., Garnett, S.T. & Woinarski, J.C. (2023) Loss of terrestrial biodiversity in Australia: Magnitude, causation, and response. *Science,* **381,** 622-631. https://www.science.org/doi/10.1126/science.adg7870

Liu, H. (2015) Comparing Welch ANOVA, a Kruskal-Wallis test, and traditional ANOVA in case of heterogeneity of variance. https://doi.org/10.25772/BWFP-YE95

Loke, L.H. & Chisholm, R.A. (2022) Measuring habitat complexity and spatial heterogeneity in ecology. *Ecology letters,* **25,** 2269-2288. https://doi.org/10.1111/ele.14084

Lundholm, J.T. (2009) Plant species diversity and environmental heterogeneity: spatial scale and competing hypotheses. *Journal of Vegetation Science,* **20,** 377-391. https://doi.org/10.1111/j.1654-1103.2009.05577.x

MacArthur, R.H. (1964) Environmental factors affecting bird species diversity. *The American Naturalist,* **98,** 387-397. https://doi.org/10.1086/282334

MacArthur, R.H., MacArthur, J.W. & Preer, J. (1962) On bird species diversity. II. Prediction of bird census from habitat measurements. *The American Naturalist,* **96,** 167-174. https://doi.org/10.1086/282219

Maestre, F.T., Cortina, J., Bautista, S., Bellot, J. & Vallejo, R. (2003) Small-scale environmental heterogeneity and spatiotemporal dynamics of seedling establishment in a semiarid degraded ecosystem. *Ecosystems,* **6,** 630-643. https://doi.org/10.1007/s10021-002-0222-5

McKight, P.E. & Najab, J. (2010) Kruskal-wallis test. *The corsini encyclopedia of psychology***,** 1-1. https://doi.org/10.1002/9780470479216.corpsy0491

Mitchell, M.G., Wu, D., Johansen, K., Maron, M., McAlpine, C. & Rhodes, J.R. (2016) Landscape structure influences urban vegetation vertical structure. *Journal of Applied Ecology,* **53,** 1477-1488. https://doi.org/10.1111/1365-2664.12741

Mori, A.S. (2020) Advancing nature-based approaches to address the biodiversity and climate emergency. *Ecology letters,* **23,** 1729-1732. https://doi.org/10.1111/ele.13594

Moudrý, V., Cord, A.F., Gábor, L., Laurin, G.V., Barták, V., Gdulová, K., Malavasi, M., Rocchini, D., Stereńczak, K. & Prošek, J. (2023) Vegetation structure derived from airborne laser scanning to assess species distribution and habitat suitability: The way forward. *Diversity and Distributions,* **29,** 39-50. https://doi.org/10.1111/ddi.13644

Naimi, B., Hamm, N.A., Groen, T.A., Skidmore, A.K., Toxopeus, A.G. & Alibakhshi, S. (2019) ELSA: Entropy-based local indicator of spatial association. *Spatial statistics,* **29,** 66-88. https://doi.org/10.1016/j.spasta.2018.10.001

Ogle, D. & Ogle, M.D. (2017) Package 'fsa'. *Cran Repos*, pp. 206.

Paul, C., Hanley, N., Meyer, S.T., Fürst, C., Weisser, W.W. & Knoke, T. (2020) On the functional relationship between biodiversity and economic value. *Science Advances,* **6,** eaax7712. https://doi.org/10.1126/sciadv.aax7712

Petruželová, J., König, S., Heurich, M., Kopáček, J., de Donnová, S., Polášková, V., Seifert, L., Šorfová, V., Sroka, P. & Straka, M. (2025) Assessing macroinvertebrate species

composition in forest streams using LiDAR-based vegetation structure variables. *Ecological Indicators,* **178,** 114088. https://doi.org/10.1016/j.ecolind.2025.114088

Poggio, S.L., Chaneton, E.J. & Ghersa, C.M. (2010) Landscape complexity differentially affects alpha, beta, and gamma diversities of plants occurring in fencerows and crop fields. *Biological Conservation,* **143,** 2477-2486. https://doi.org/10.1016/j.biocon.2010.06.014

Pohlert, T. & Pohlert, M.T. (2018) Package 'pmcmr'. *R package version,* **1.** https://doi.org/10.32614/CRAN.package.PMCMRplus

Pottier, J., Bédécarrats, A. & Marrs, R.H. (2009) Analysing the spatial heterogeneity of emergent groups to assess ecological restoration. *Journal of Applied Ecology,* **46,** 1248-1257. https://doi.org/10.1111/j.1365-2664.2009.01714.x

R Core Team, R. (2023) *R: A language and environment for statistical computing***,** Vienna, Austria: R Foundation for Statistical Computing

Ranjard, L., Dequiedt, S., Chemidlin Prévost-Bouré, N., Thioulouse, J., Saby, N., Lelievre, M., Maron, P., Morin, F., Bispo, A. & Jolivet, C. (2013) Turnover of soil bacterial diversity driven by wide-scale environmental heterogeneity. *Nature communications,* **4,** 1434.https://doi.org/10.1038/ncomms2431

Rescia, A., Schmitz, M., Martin de Agar, P., De Pablo, C. & Pineda, F.D. (1997) A fragmented landscape in northern Spain analyzed at different spatial scales: implications for management. *Journal of Vegetation Science,* **8,** 343-352.https://doi.org/10.2307/3237323

Sarr, D.A., Hibbs, D.E. & Huston, M.A. (2005) A hierarchical perspective of plant diversity. *The quarterly review of biology,* **80,** 187-212.https://doi.org/10.1086/433058

Schindler, S., Poirazidis, K. & Wrbka, T. (2008) Towards a core set of landscape metrics for biodiversity assessments: a case study from Dadia National Park, Greece. *Ecological Indicators,* **8,** 502-514.https://doi.org/10.1016/j.ecolind.2007.06.001

Seidel, D. (2018) A holistic approach to determine tree structural complexity based on laser scanning data and fractal analysis. *Ecology and evolution,* **8,** 128-134.https://doi.org/10.1002/ece3.3661

Seiferling, I., Proulx, R. & Wirth, C. (2014) Disentangling the environmental-heterogeneity–species-diversity relationship along a gradient of human footprint. *Ecology,* **95,** 2084-2095.https://www.jstor.org/stable/43494716

Shen, W., Darrel Jenerette, G., Wu, J. & H. Gardner, R. (2004) Evaluating empirical scaling relations of pattern metrics with simulated landscapes. *Ecography,* **27,** 459-469.https://doi.org/10.1111/j.0906-7590.2004.03799.x

Shi, Y., Wang, J. & Kissling, W.D. (2025) Multi-temporal high-resolution data products of ecosystem structure derived from country-wide airborne laser scanning surveys of the Netherlands. *Earth System Science Data,* **17,** 3641-3677.https://doi.org/10.5194/essd-17-3641-2025

Shin, Y.J., Midgley, G.F., Archer, E.R., Arneth, A., Barnes, D.K., Chan, L., Hashimoto, S., Hoegh-Guldberg, O., Insarov, G. & Leadley, P. (2022) Actions to halt biodiversity loss generally benefit the climate. *Global change biology,* **28,** 2846-2874.https://doi.org/10.1111/gcb.16109

Siefert, A., Ravenscroft, C., Althoff, D., Alvarez-Yépiz, J.C., Carter, B.E., Glennon, K.L., Heberling, J.M., Jo, I.S., Pontes, A. & Sauer, A. (2012) Scale dependence of vegetation–

environment relationships: a meta-analysis of multivariate data. *Journal of Vegetation Science,* **23,** 942-951.https://doi.org/10.1111/j.1654-1103.2012.01401.x

Simpson, E.H. (1949) Measurement of diversity. *Nature,* **163,** 688-688.https://doi.org/10.1038/163688a0

Smith, T.W. & Lundholm, J.T. (2012) Environmental geometry and heterogeneity–diversity relationships in spatially explicit simulated communities. *Journal of Vegetation Science,* **23,** 732-744.https://doi.org/10.1111/j.1654-1103.2011.01380.x

Stein, A. (2015) Environmental heterogeneity–species richness relationships from a global perspective. *Frontiers of Biogeography,* **7,** 168-173.https://api.semanticscholar.org/CorpusID:55551803

Stein, A., Gerstner, K. & Kreft, H. (2014) Environmental heterogeneity as a universal driver of species richness across taxa, biomes and spatial scales. *Ecology Letters,* **17,** 866-880.https://doi.org/10.1111/ele.12277

Stein, A. & Kreft, H. (2015) Terminology and quantification of environmental heterogeneity in species-richness research. *Biological Reviews,* **90,** 815-836.https://doi.org/10.1111/brv.12135

Tews, J., Brose, U., Grimm, V., Tielbörger, K., Wichmann, M.C., Schwager, M. & Jeltsch, F. (2004) Animal species diversity driven by habitat heterogeneity/diversity: the importance of keystone structures. *Journal of biogeography,* **31,** 79-92.https://doi.org/10.1046/j.0305-0270.2003.00994.x

Trevail, A.M., Green, J.A., Bolton, M., Daunt, F., Harris, S.M., Miller, P.I., Newton, S., Owen, E., Polton, J.A. & Robertson, G. (2021) Environmental heterogeneity promotes

individual specialisation in habitat selection in a widely distributed seabird. *Journal of Animal Ecology,* **90,** 2875-2887.https://doi.org/10.1111/1365-2656.13588

Van Rensburg, B., Chown, S. & Gaston, K. (2002) Species richness, environmental correlates, and spatial scale: a test using South African birds. *The American Naturalist,* **159,** 566-577.https://doi.org/10.1086/339464

Weisberg, P.J., Dilts, T.E., Becker, M.E., Young, J.S., Wong-Kone, D.C., Newton, W.E. & Ammon, E.M. (2014) Guild-specific responses of avian species richness to LiDAR-derived habitat heterogeneity. *Acta Oecologica,* **59,** 72-83.https://doi.org/10.1016/j.actao.2014.06.002

Wiens, J.A. (1989) Spatial scaling in ecology. *Functional ecology,* **3,** 385-397.https://doi.org/10.2307/2389612

Worm, B., Barbier, E.B., Beaumont, N., Duffy, J.E., Folke, C., Halpern, B.S., Jackson, J.B., Lotze, H.K., Micheli, F. & Palumbi, S.R. (2006) Impacts of biodiversity loss on ocean ecosystem services. *Science,* **314,** 787-790.https://doi.org/10.1126/science.1132294

1 **Tables**

2 Table 1: Characteristics of measures used for calculating vegetation heterogeneity

VH measures	Unit	Description	Datasets	Resolution	Data type
Mean vegetation height (MEV)	m	Mean height of vegetation within the cell	AHN3 product	0.01 km	LiDAR data
Vegetation absolute height (VAH)	m	Height categories: (1<, 1-2, 2-3, 3-4, 4-5, 5-20, >20)	AHN3 product	0.01 km	LiDAR data
Vegetation foliage layer (VF)	m	Functional vegetation layers (tall trees, trees, shrubs, grass)	AHN3 product	0.01 km	LiDAR data
Vegetation openness (VO)	%	Ratio of number of ground points to total number of points within a cell	AHN3 product	0.01 km	LiDAR data
Canopy cover (CC)	-	Returns above mean height per cell	AHN3 product	0.01 km	LiDAR data
Maximum vegetation height (MAV)	m	Maximum height of the vegetation surface	AHN3 product	0.01 km	LiDAR data
Vegetation species number (VS)	-	Number of vascular plant species	NDFF	0.01 km	Observation data

3 *Note:* AHN3 represents dataset: Actueel Hoogtebestand Nederland version 3. NDFF

4 represents the dataset: Nationale Databank Flora en Fauna. LiDAR data is the Light

5 Detection and Ranging data.

6

Table 2 Shape of vegetation heterogeneity change across spatial scales using seven measures, three methods, and across three landscape types

Landscape type	**Urban**			**Agricultural**			**Simi-natural**		
Method	CV	SD	H'	CV	SD	H'	CV	SD	H'
Mean vegetation height (MEV)	NL-L	NL-P	NL-P	NL-P	NL-L	NL-L	NL-L	NL-L	NL-L
Vegetation absolute height (VAH)	NL-P	NL-P	L+	NL-L	NL-L	NL-L	L+	NL-L	NL-L
Vegetation foliage layer (VF)	NL-L	NL-L	NL-P	L+	NL-L	L+	NL-P	NL-L	NL-L
Vegetation openness (VO)	L+	NL-P	L+	NL-L	NL-L	NL-L	NL-L	NL-L	NL-P
Canopy cover (CC)	NL-L	NL-L	NL-P	NL-L	NL-L	NL-L	NL-L	NL-L	NL-L
Maximum vegetation height (MAV)	NL-L	NL-P	NL-P	NL-L	NL-L	NL-L	NL-L	NL-L	NL-L
Vegetation species (VS)	L+	NL-L		NL-P	NL-L		NL-P	NL-L	

Note: Three methods have been used for vegetation heterogeneity: Coefficient of variation (CV), Standard deviation (SD), and Shannon's diversity index (H'). Landscape types has been considered in the calculation: urban, agricultural, and simi-natural landscape. "L+" represents positive linear relationships, and "L-" for negative linear relationships. "NL-L" for logarithmic nonlinear trends, "NL-P" for polynomial nonlinear trends.

Figure legends

Fig. 1 Hypothetical patterns of environmental heterogeneity across spatial scales. (I) Positive linear; (II) Negative linear; (III) Hump-shaped polynomial; (IV) U-shaped polynomial; (V) Positive logarithmic; (VI) Negative logarithmic.

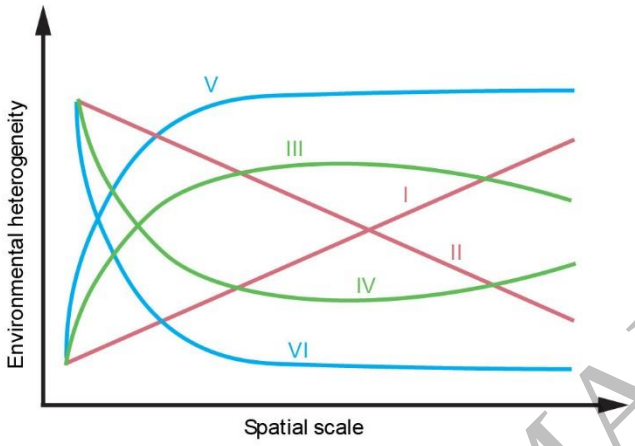

Fig. 2 Agricultural, urban, and semi-natural landscapes are derived from the Landelijk Grondgebruik Nederland (LGN) 2018 (see Supplementary Table S1, for the classification scheme).

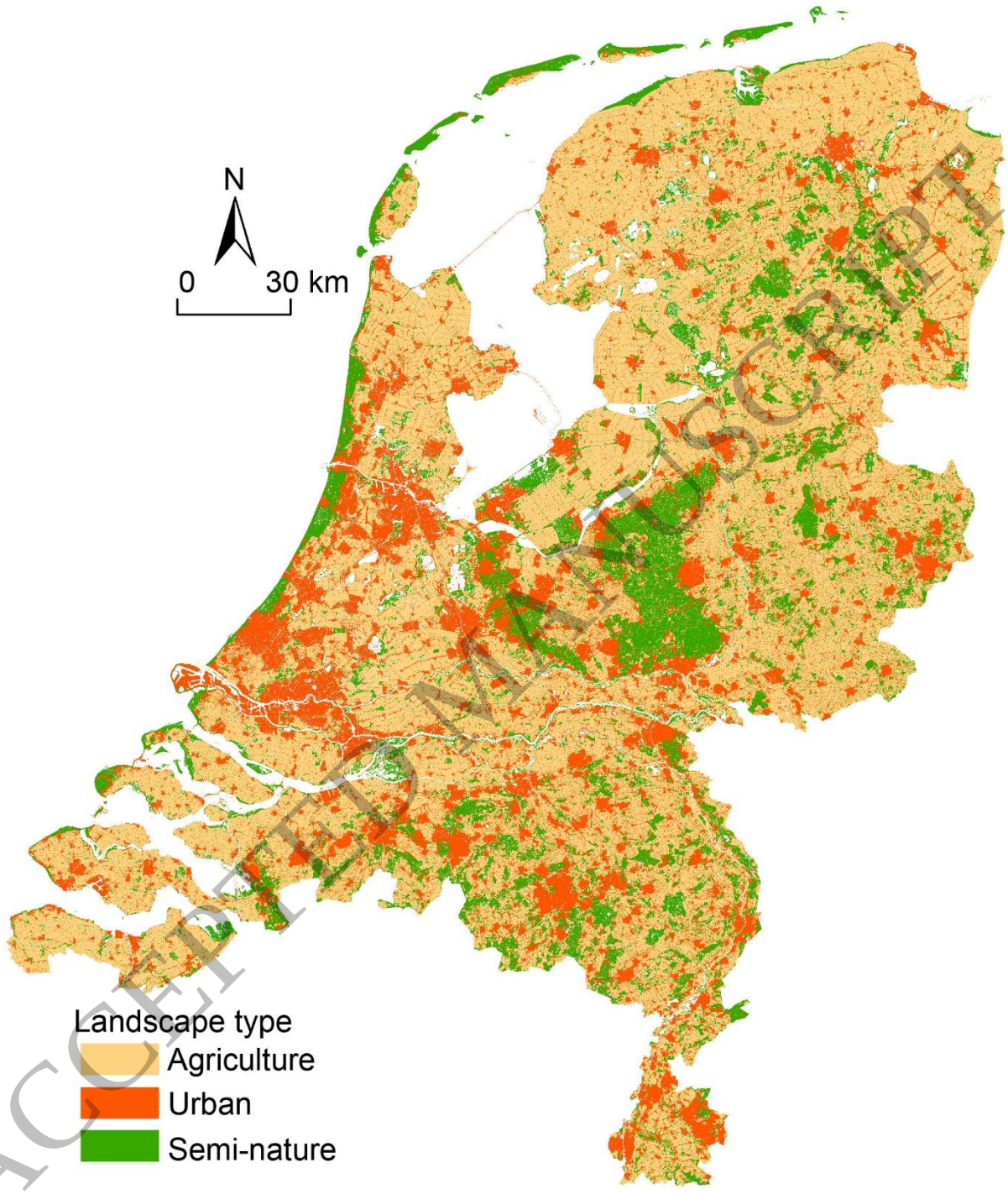

1

2

Fig. 3 Conceptual illustration of the vegetation heterogeneity measures used in this study. Six measures were derived from LiDAR data: vegetation foliage layer, vegetation absolute height, canopy cover, vegetation openness, mean vegetation height, and maximum vegetation height. Vegetation species heterogeneity was derived from field observation data. Vegetation foliage layer represents the vertical stratification of vegetation into grass, shrubs, trees, and tall trees, whereas vegetation absolute height describes vegetation structure using discrete height classes. Mean vegetation height and maximum vegetation height represent the average and tallest vegetation height within a sampling unit, respectively. Canopy cover was calculated as the number of returns above mean height within a cell, and vegetation openness as the ratio of ground points to total points within a cell. Vegetation species heterogeneity represents variation in plant species composition based on field observations.

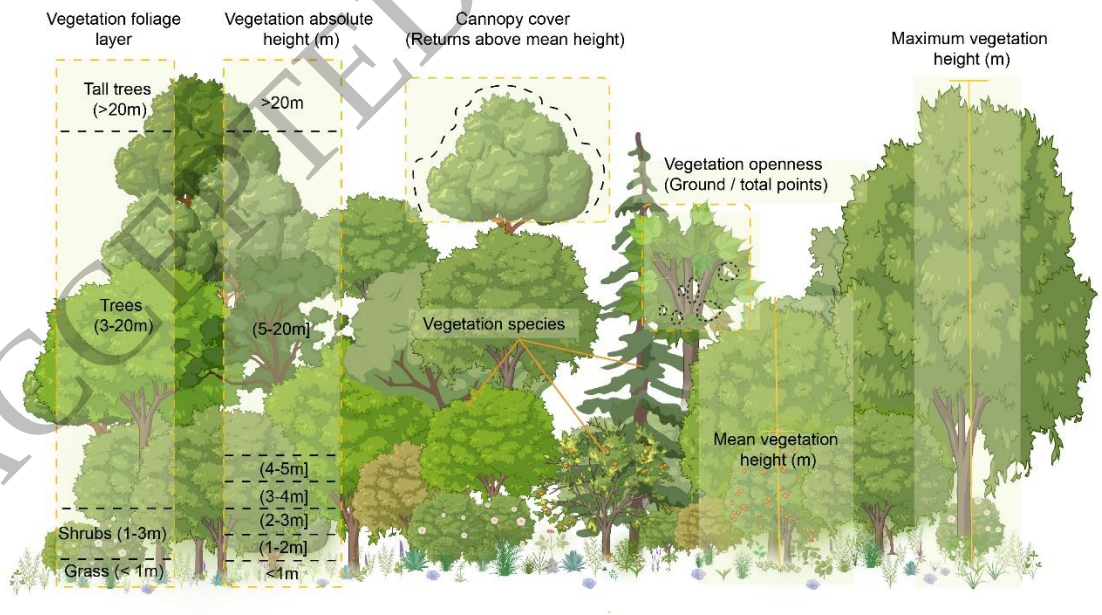

Fig. 4 Relationships between vegetation heterogeneity and spatial scale across urban (A), agricultural (B), and semi-natural (C) landscapes. Rows represent vegetation heterogeneity measures (MEV, VAH, VF, VO, CC, MAV, and VS), and columns represent calculation methods (CV, SD, and SI). Blue points show the mean observed heterogeneity value at each spatial grain across 99 resampling iterations. Colored lines show the best- supported model for each dataset, selected as the model with the highest mean Akaike weight across iterations: linear (red), logarithmic (blue), and second-degree polynomial (green). The vertical black dashed line marks 0.5 km. X-axis values are shown in kilometres. Supplementary Fig. S31 presents the corresponding plots with standard deviations among iterations, and Supplementary Fig. S 25-32 provides an enlarged view of the ≤ 0.5 km range.

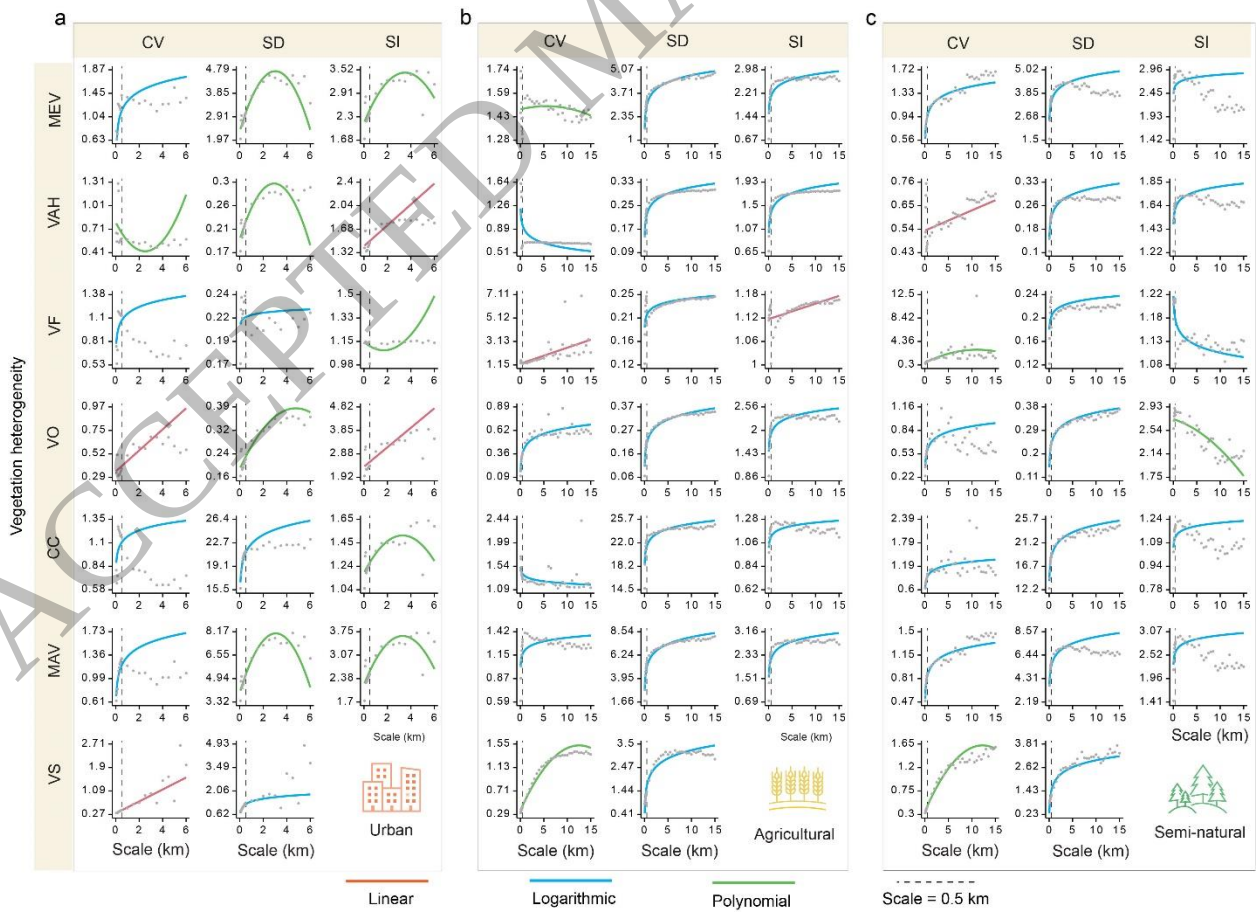

Fig. 5 Differences in maximum slope among vegetation heterogeneity measures (A), heterogeneity calculation methods (B), and landscape types (C). Boxplots are based on the mean maximum absolute slope across 99 iterations for datasets in which a nonlinear model (logarithmic or polynomial) received the strongest support, and the y-axis shows these values on the original (untransformed) scale. The maximum slope was defined as the maximum absolute slope estimated from the best-supported model. Centre lines show medians, boxes show interquartile ranges, and whiskers show the range excluding outliers. P-values are from Kruskal–Wallis tests, and different letters denote significant differences among groups based on Dunn's post hoc comparisons. Abbreviations: MEV, mean vegetation height; VAH, vegetation absolute height; VF, vegetation foliage layer; VO, vegetation openness; CC, canopy cover; MAV, maximum vegetation height; VS, vegetation species heterogeneity; CV, coefficient of variation; SD, standard deviation; SI, Shannon index.

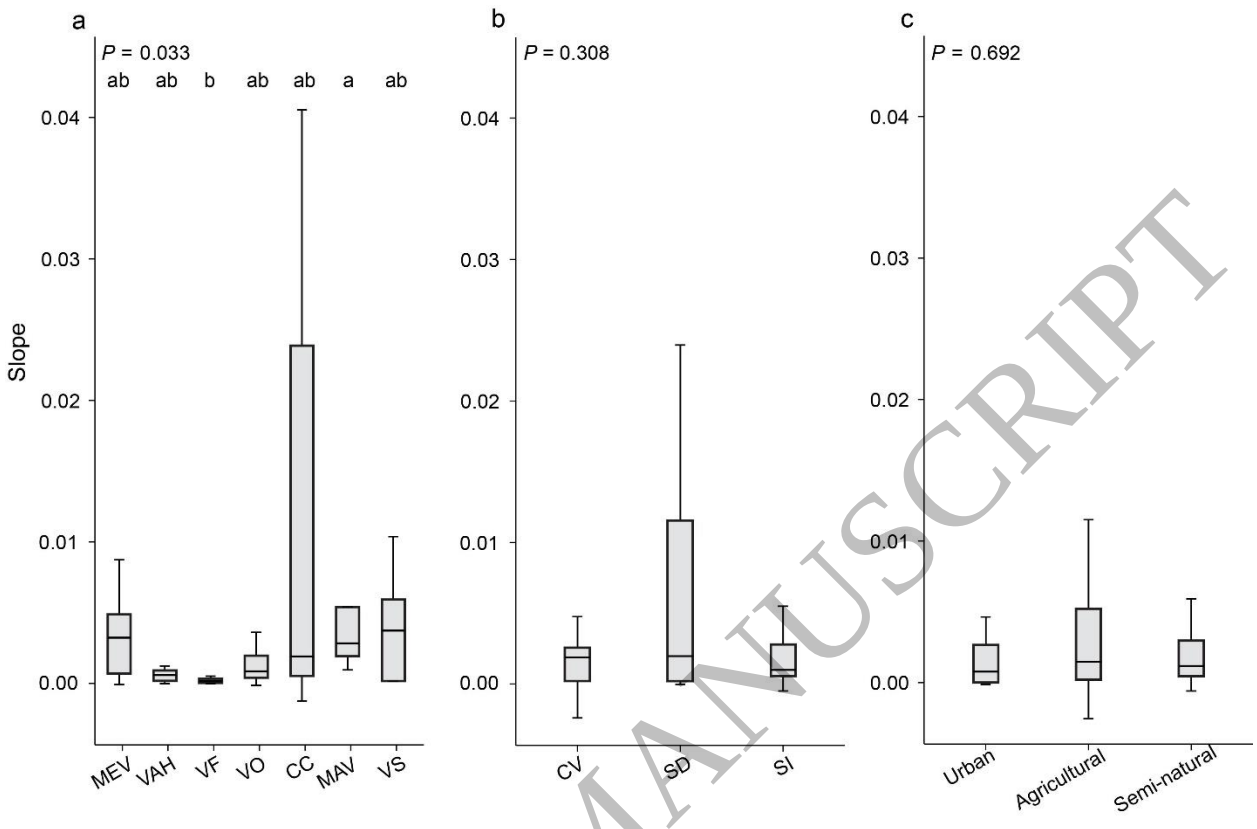

Fig. 6 Differences in levelling-off scale among vegetation heterogeneity measures (A), heterogeneity calculation methods (B), and landscape types (C). Boxplots are based on the mean levelling-off scale across 99 iterations for datasets in which the logarithmic model received the strongest support, and the y-axis shows these values on the original (untransformed) scale. The levelling-off scale was defined as the spatial scale at which the predicted response reached 95% of its maximum. Centre lines show medians, boxes show interquartile ranges, and whiskers show the range excluding outliers. P-values are from Kruskal–Wallis tests, and different letters denote significant differences among groups based on Dunn's post hoc comparisons. Abbreviations: MEV, mean vegetation height; VAH, vegetation absolute height; VF, vegetation foliage layer; VO, vegetation openness; CC,

canopy cover; MAV, maximum vegetation height; VS, vegetation species heterogeneity; CV, coefficient of variation; SD, standard deviation; SI, Shannon index.

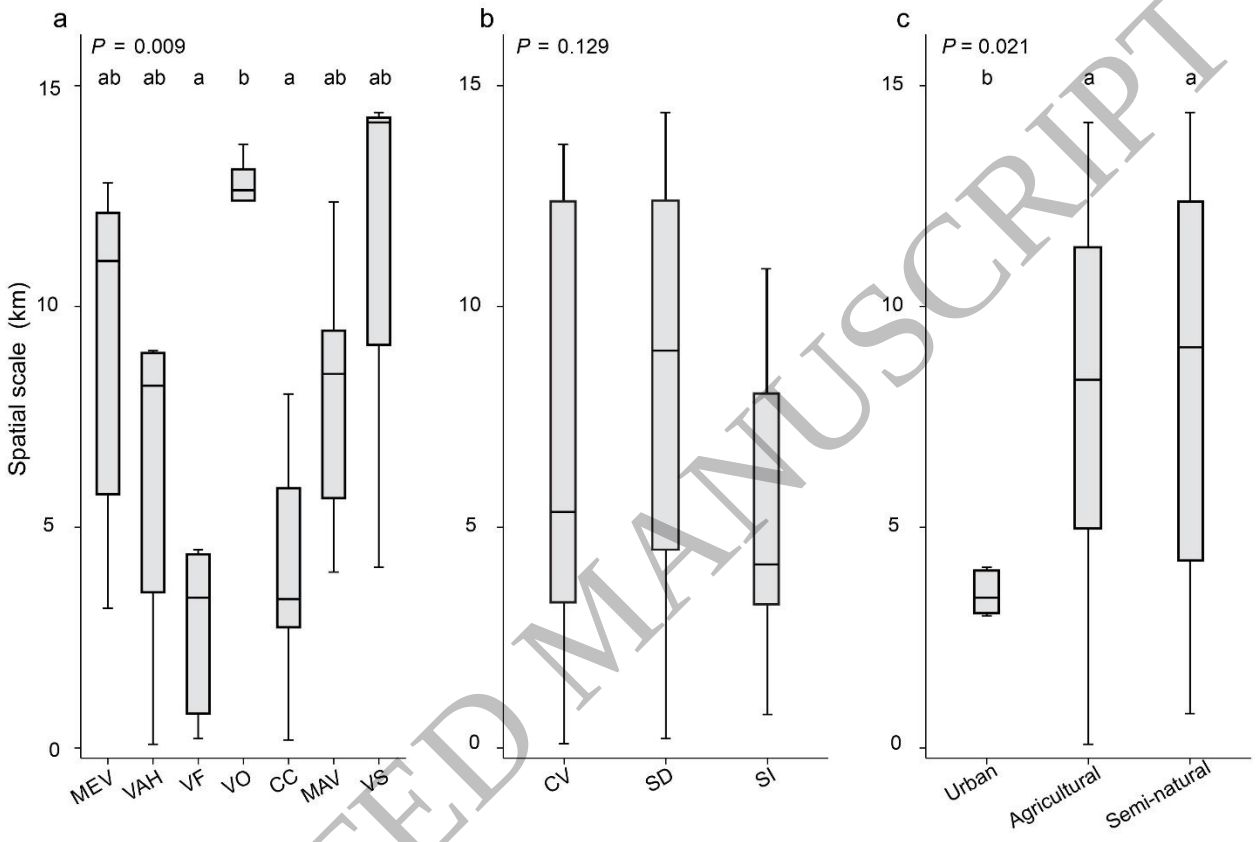

1 Graphical Abstract

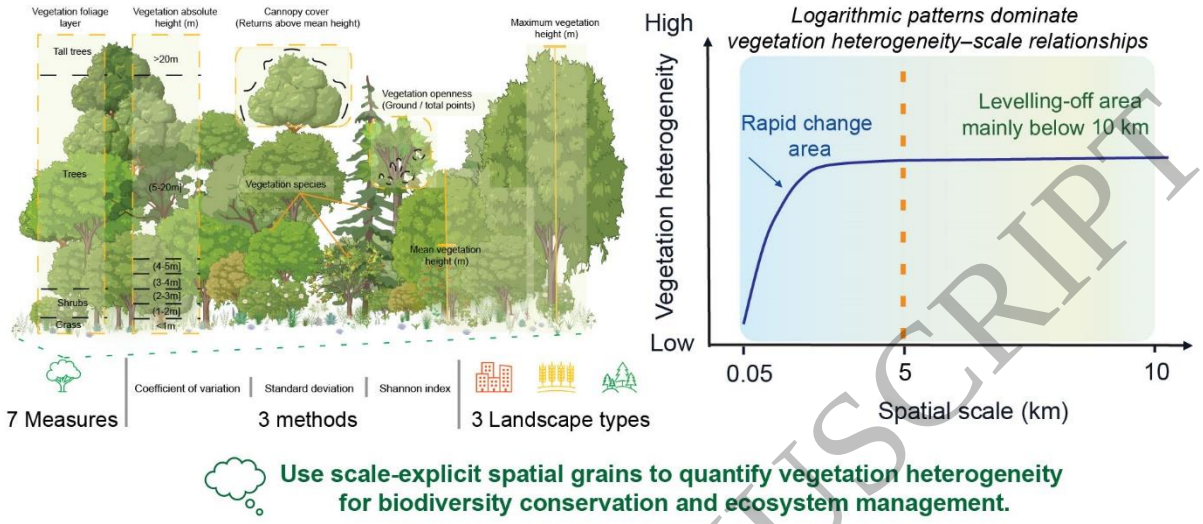

2